

# Equivalent Signal Theory for Frequency Domain Modeling of Linear Time-Periodic Systems: PWM Application

Mohamed Abdel-Rahman, Abner Ramirez

**Abstract**— Equivalent Signal Theory proves that a sampled signal can be represented by a synthetic continuous function on the condition that this synthetic function coincides with a sampling of a signal at the sampling times and is limited by the bandwidth of the original input signal. The result of this theory, in general terms, is the possibility to develop special type of Frequency-Domain (FD) transfer functions among a train of sampled inputs and a train of sampled outputs, termed Generalized Transfer Functions (GTFs). For a switched power network, while the input is a continuous function the output may be considered as a piece-wise continuous function. This paper investigates analytically the application of this theory to obtain an input-output FD relationship for a PWM switched converter. It further looks into the direct application of Vector Fitting as a short and more convenient way to present those GTFs. The developed models are verified by Time-Domain (TD) simulation.

**Keywords**—Frequency-domain analysis, signal analysis, switched circuits, transfer functions.

## I. INTRODUCTION

Time-domain (TD) modeling and simulation of power systems that include periodically switched converters achieve high accuracy when using different platforms from the electromagnetic transient (EMT) program family [1], [2]. This accuracy comes at the cost of relatively lengthy simulation times. Furthermore, fixed-step TD simulation has its own limitations in treating switching converters for cases where the switching instant does not coincide with the time-step, which may lead to fictitious frequencies in the simulation result [3]. Enhanced fixed-step methods, e.g., using interpolation, and variable time-step approaches, have not completely overcome long simulation times and use of large computational resources when applied to switched networks.

A well-established alternative for a full-fledged TD simulation of switched devices is the time-averaging models [4], [5]. Averaged models fill the gap for both motor control

and power supply applications. Nonetheless, averaged models do not capture the periodically switched system's dynamics. The model may easily miss the presence of resonance within the frequency band-width of the studied phenomenon.

On the other hand, FD is the preferred domain for linear time-invariant (LTI) systems analysis and has served for verification of new TD models. However, pure FD techniques have not evolved to the point of facilitating simulation of periodically time-varying systems, e.g., switched devices. The inability to use FD techniques deprived analysts from the use of available FD tools for many applications, e.g., stability analysis.

Among FD techniques is the dynamic harmonic domain (DHD) approach [6], from which the harmonic domain dynamic transfer function (HDDTF) concept is generated [7]. The HDDTF relates the frequency spectra vectors of input and output signals. No equivalent signals are involved in DHD-based approaches.

Equivalent Signal Theory, developed by Tsvividis, was utilized by Birolek to build a special type of transfer functions for a periodically switched linear network, the Generalized Transfer Functions (GTFs). These special functions provide FD relationship between the equivalent signals, as defined by the equivalent signal theory, and the input [8]. The properties of the replacing equivalent signal are: a) the equivalent and output signals have common points at sampling instances and b) the spectral components of the equivalent signal fall into the spectral area of the input signal [9]. The importance of this theory relies in the fact that GTFs simultaneously describe continuous-time ( $s$ -domain) and discrete-time ( $z$ -domain) input/output characteristics of a switched network [9]-[14]. It is mentioned that  $z$ -domain poles are decisive for system stability while  $s$ -domain poles define system's transient behavior. Mathematical complexity of the approach hindered its widespread application for switched circuits, reporting at most two-switching phase cases in specialized literature [9]-[14]. A great deal of effort has been dedicated to addressing the numerical task of simulating GTFs in semi-symbolic ways [9]-[14].

Computing the complete spectrum of a switched device can be computationally expensive. GTFs provide an alternative of characterizing a switched device in FD via equivalent signals. Also, GTFs permit to model system's behavior more accurately than averaged models and classical  $s$ -domain zeros/poles location, including special effects above Nyquist's

---

This work was supported in part by SENER-CONACYT under project 246949.

M. A. Abdel-Rahman is with Electrical Power and Machines Engineering Department, Faculty of Engineering, Ain Shams University, Cairo, Egypt (e-mail: [mohamed\\_a\\_rahman@eng.asu.edu.eg](mailto:mohamed_a_rahman@eng.asu.edu.eg))

A. Ramirez is with CINVESTAV campus Guadalajara, Mexico, 45019 (e-mail: [abner.ramirez@cinvestav.mx](mailto:abner.ramirez@cinvestav.mx)).

frequency [11].

In this context, this paper applies Equivalent Signal Theory to deduce analytically a model for a Half Bridge Converter (HBC) under full-wave and PWM switching schemes. It is demonstrated that the employment of existent numerical techniques, such as the numerical Laplace transform (NLT) [15], overcomes the issue of numerical complexity which has limited GTF application to two-switching phase case. As shown in the paper, GTFs give access to zeros/poles in both  $s$ - and  $z$ -domain as means of evaluating stability and dynamics of the device under analysis. Moreover, Vector Fitting is used to provide a simpler expression of the GTF, limited to the  $s$ -domain. The adopted approach enables spectral analysis of the switched circuit. The ability to identify poles and zeros location for a switched system provides system designers of an educated guess of the actual system performance. In addition, the paper provides a thorough analysis of the HBC case from distinct points of view such as frequency-domain and state-space realizations to facilitate computational comprehension of implementation. This is a novel application of the methodology that was not achieved earlier than this effort, neither for this network topology nor for the studied switching pattern.

## II. EQUIVALENT SIGNAL THEORY

Consider a momentarily switched system with a switching period  $T$  and a duty cycle  $d$ , driven by input  $x(t)$  and providing output  $y(t)$ . The output  $y(t)$  is sampled at instants  $kT + dT$  that correspond to the starting of a switching phase, at the end of a switching phase, or at any arbitrary point after the end of a switching phase. We define the equivalent signal  $y_d^e(t)$  of the sequence  $y\{kT + dT\}$ ,  $k = \dots, -1, 0, 1, \dots$  as the signal that satisfies two properties, viz.,

a) Represents interpolation of the sequence  $y\{kT + dT\}$ ,  $k = \dots, -1, 0, 1, \dots$ . That is, the equivalent signal and the instantaneous output are the same at sampling points  $kT + dT$ .

b) Has frequency components within the spectrum of  $x(t)$ . This means that  $y_d^e(t)$  is identical to  $y(t)$  if the Nyquist's criterion is satisfied, i.e.,  $f_{\max} = 1/(2T)$ , where  $f_{\max}$  represents the maximum frequency component of  $y(t)$ . An equivalent signal for the input  $x^e(t)$ , can be defined accordingly.

It is noted that construction of equivalent signals depends on parameter  $d$ ; thus, a family of envelopes of  $y_d^e(t)$  can be defined. The GTF representing input/output equivalent signal's relationship is given by ( $\mathbf{L}$  represents Laplace transform operator)

$$GTF_d = \mathbf{L}\{y_d^e(t)\} / \mathbf{L}\{x^e(t)\} = \mathbf{L}\{y_d^e(t)\} / \mathbf{L}\{x(t)\}, \quad (1)$$

where the term at the outmost right applies when  $x(t)$  satisfies the Nyquist's criterion.

It is shown in [9]-[14] that GTFs are capable of simultaneously describing  $s$ - and  $z$ -domain characteristics of switched circuits. Therefore, the double substitution,  $s = j\omega$

and  $z = e^{j\omega T}$ , permits to analyze their frequency response. Furthermore, since GTFs are functions of both  $s$  and  $z$ , zeros/poles characteristics of the switched circuit can be derived for both domains [9].

## III. PROPOSED MODELING

Consider the HBC depicted in Fig. 1a, noting that ideal switches are assumed in this paper [5], [16]. Fig. 1b depicts  $v_{out}(t)$ , assuming the switching pattern as given by PWM scheme. The fundamental period of time  $T$  is partitioned into  $N$  switching phases, satisfying

$$\sum_{i=1}^N d_i T = T, \quad (2)$$

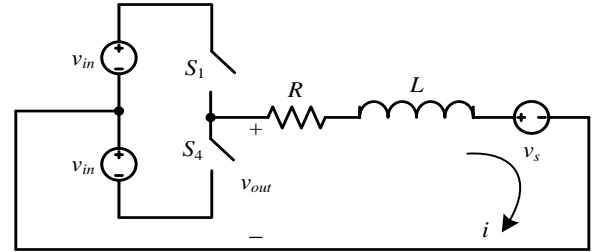
where  $d_i$  is the duty cycle ratio. It is noted that the network changes its topology due to switching from one switching phase to the next.

Consider the first two topology changes of the HBC. For the first switching phase, i.e., when  $S_1$  is on and  $S_4$  is off, we have the TD relation:

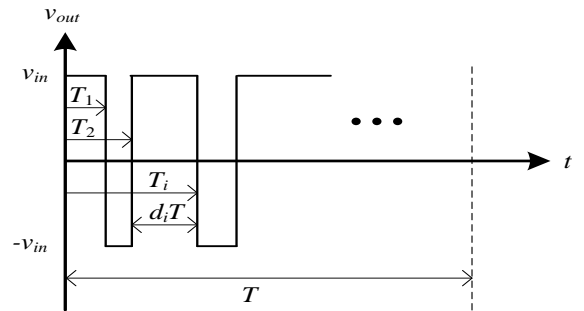
$$L \frac{di_1}{dt} + Ri_1 = v_{in}(t) - v_s(t). \quad (3a)$$

Similarly, for the second switching phase, i.e., when  $S_1$  is off and  $S_4$  is on, we have:

$$L \frac{di_2}{dt} + Ri_2 = -v_{in}(t) - v_s(t). \quad (3b)$$



(a)



(b)

**Fig. 1.** (a) Half-bridge converter and (b) Associated voltage output waveform corresponding to PWM scheme.

Applying the Laplace transform to (3a) and (3b) yields

$$(R + sL)I_1(s) = Li_1(0) + V_{in}(s) - V_s(s), \quad (4a)$$

$$(R + sL)I_2(s) = Li_2(0) - V_{in}(s) - V_s(s). \quad (4b)$$

Extending (4) to the defined  $N$ -switching phases case and rearranging in matrix format results in:

$$\begin{bmatrix} R+sL & 0 & \cdots & 0 \\ 0 & R+sL & \ddots & \vdots \\ \vdots & \vdots & \ddots & 0 \\ 0 & \cdots & 0 & R+sL \end{bmatrix} \begin{bmatrix} I_1(s) \\ I_2(s) \\ \vdots \\ I_N(s) \end{bmatrix} = \begin{bmatrix} 0 & \cdots & 0 & L \\ L & 0 & \ddots & \vdots \\ \vdots & \vdots & \ddots & 0 \\ 0 & 0 & L & 0 \end{bmatrix} \begin{bmatrix} i_1(kT+T) \\ i_2(kT+T_1) \\ \vdots \\ i_N(kT+T_{N-1}) \end{bmatrix} + V_{in} \begin{bmatrix} 1 \\ -1 \\ \vdots \\ (-1)^{N-1} \end{bmatrix} - V_s \begin{bmatrix} 1 \\ \vdots \\ 1 \end{bmatrix}, \quad (5)$$

where  $I_i(s)$  corresponds to the FD current during the  $i$ th time switching phase and  $i_i(kT+T_i)$  is the initial value of the current at instant  $kT+T_i$ . Replacing  $i_i(kT+T_i)$  by an equivalent (time-continuous) signal,

$$i_i(kT+T_i) = i_i^e(t-d_iT), \quad (6)$$

where superscript  $e$  denotes equivalent. Therefore, (5) becomes in the TD [10]:

$$\begin{aligned} i_1^e(t) &= i_N^e(t-d_1T)e^{-d_1T/\tau} + e^{-t/\tau} * \mathbf{L}^{-1}\{V_{in}(s)-V_s(s)\}/L \\ i_2^e(t) &= i_2^e(t-d_2T)e^{-d_2T/\tau} + e^{-t/\tau} * \mathbf{L}^{-1}\{-V_{in}(s)-V_s(s)\}/L, \quad (7) \\ &\vdots \end{aligned}$$

where  $*$  stands for convolution operation and  $\tau = L/R$ . Finally, taking the Laplace transform of (7) yields (using the substitution  $z = e^{sT}$ )

$$\begin{bmatrix} 1 & 0 & \cdots & -g_1z^{-d_1} \\ -g_2z^{-d_2} & 1 & \ddots & 0 \\ \vdots & \vdots & \ddots & \vdots \\ 0 & 0 & \cdots & 1 \end{bmatrix} \begin{bmatrix} I_1^e \\ I_2^e \\ \vdots \\ I_N^e \end{bmatrix} = \begin{bmatrix} G_1 \cdot (V_{in} - V_s) \\ G_2 \cdot (-V_{in} - V_s) \\ \vdots \\ G_N \cdot [(-1)^{N-1}V_{in} - V_s] \end{bmatrix}, \quad (8)$$

where:  $G_i = (1/L) \frac{1-z^{-d_i}e^{-d_iT/\tau}}{s+1/\tau}$  and  $g_i = e^{-d_iT/\tau}$ .

The set of the  $N$  equivalent signals in (8) depends on parameter  $d_i$  and can be visualized as TD envelopes of  $I(s)$ . According to the equivalent signal theory, an equivalent signal is equal to the sampled signal at points  $kT+T_i$  [8].

#### IV. SPECIAL CASE: TWO-SWITCHING PHASE HBC

To numerically illustrate the HBC model outlined in the previous subsection, consider the two-switching phase case or full-wave switching,  $N=2$ , with duty ratio equal to  $d$ . For this special case, (8) becomes

$$\begin{bmatrix} 1 & -g_1e^{-dT/\tau} \\ -g_2e^{-T(1-d)s} & 1 \end{bmatrix} \begin{bmatrix} I_1^e \\ I_2^e \end{bmatrix} = \begin{bmatrix} G_1(V_{in}-V_s) \\ G_2(-V_{in}-V_s) \end{bmatrix}, \quad (9)$$

where:

$$G_1 = (1/L) \frac{1-g_1e^{-dT/\tau}}{s+1/\tau}, \quad G_2 = (1/L) \frac{1-g_2e^{-T(1-d)s}}{s+1/\tau}$$

and

$$g_1 = e^{-dT/\tau}, \quad g_2 = e^{-T(1-d)/\tau}$$

The GTFs of the two-switching phase HBC are obtained from (9) resulting in:

$$\begin{bmatrix} I_1^e \\ I_2^e \end{bmatrix} = \begin{bmatrix} GTF_{11} & GTF_{12} \\ GTF_{21} & GTF_{22} \end{bmatrix} \begin{bmatrix} V_{in} \\ V_s \end{bmatrix}, \quad (10)$$

where:

$$\begin{aligned} GTF_{11} &= -\frac{G_1+a_1G_2}{a_1a_2-1}, & GTF_{12} &= \frac{G_1-a_1G_2}{a_1a_2-1}, \\ GTF_{21} &= \frac{G_2+a_2G_1}{a_1a_2-1}, & GTF_{22} &= \frac{G_2-a_2G_1}{a_1a_2-1}, \end{aligned}$$

and

$$a_1 = -g_1e^{-dT/\tau}, \quad a_2 = -g_2e^{-T(1-d)/\tau}$$

Consider the following parameters:  $L = 690 \mu\text{H}$ ,  $R = 5 \text{ m}\Omega$ ,  $v_{in} = 1200 \text{ V}$ ,  $v_s = 400 \text{ V}$ ,  $d = 0.84$ , switching frequency  $f_s = 1620 \text{ Hz}$  ( $T_s = 617 \mu\text{s}$ ), and zero initial conditions. Numerical results follow.

##### a) FD characterization

The magnitude and phase of the four GTFs in (10) are presented in Fig. 2 for a frequency range of 1 Hz to 20 kHz. Fig. 2a shows that the first spike appears around the switching frequency, i.e., 1.62 kHz, and subsequent spikes appear around integer multiples of the switching frequency.

The obtained GTFs capture the system dynamics including switching and can be characterized by  $s$ - and  $z$ -domain zero/pole location; for the two-switching phase HBC case these are presented in Table I, numerical values indicated within parentheses. The zeros/poles of Table I are obtained by evaluating the corresponding GTFs using the substitution  $z = e^{j\omega T}$  and based on values  $g_1 = 0.9962$  and  $g_2 = 0.9993$ , obtained from the assumed HBC parameters.

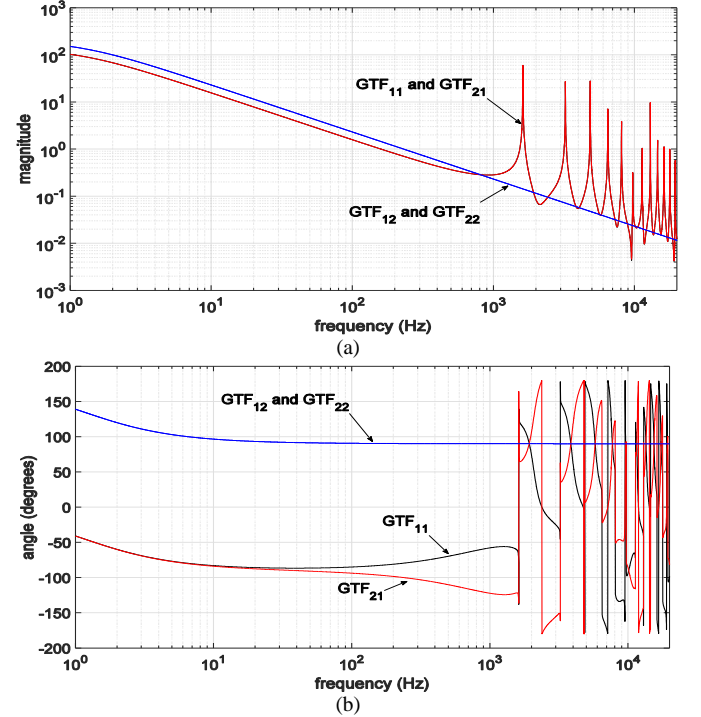


Fig. 2. GTFs of two-switching phase HBC (a) Magnitudes and (b) Phases.

It should be noted that the GTF characterization of the 2-phase HBC, as shown in Fig. 2 and Table I, corresponds to open-loop behavior. Nonetheless, it sets a basis for stability analysis and control design.

##### b) TD verification

A major feature of the equivalent signal theory is that an input/output relation can be obtained via GTFs, as in (10). This property of GTFs is utilized in this section to verify and validate the model. Note again that, at this stage of research, the case studies presented in this paper assume open-loop

simulation. This means that switching dynamics are limited to a fixed operating point.

TABLE I  
ZEROS/POLES OF HBC: TWO-SWITCHING PHASE CASE

GTF	s-domain		z-domain	
	zeros	poles	zeros	poles
$GTF_{11}$	–	$-1/\tau$ (-7.2464)	Roots of: $1 + g_1 g_2 z^{-1} - 2g_1 z^{-d} = 0$ (0.0143)	$g_1 g_2$ (0.9955)
$GTF_{12}$	–	$-1/\tau$ (-7.2464)	$g_1 g_2$ (0.9955)	$g_1 g_2$ (0.9955)
$GTF_{21}$	–	$-1/\tau$ (-7.2464)	Roots of: $1 + g_1 g_2 z^{-1} - 2g_2 z^{-d-1} = 0$ (0.9955)	$g_1 g_2$ (0.9955)
$GTF_{22}$	–	$-1/\tau$ (-7.2464)	$g_1 g_2$ (0.9955)	$g_1 g_2$ (0.9955)

In this paper, which puts forward the theory of GTFs together with its underlying principle of equivalent theory as a means to analyze power converters, comparison of the developed model to the detailed TD model is adequate for the developed model verification. TD models are well established and may be utilized to validate control and other modelling methodologies. Experimental verification of the proposed GTFs method in improving the power converter circuit/parameter design/adjustment is beyond the main objective and left for a future publication.

Next, the two-switching phase HBC GTF model is simulated to analyze its transient characteristics and is compared to a base model. This is achieved in the following manner: i) a switching-based time-domain (SW-TD) base model in which the ordinary differential equations (ODEs) (3) are solved directly in TD, ii) an FD model that uses the numerical Laplace transform (NLT) [15] to solve (10), and iii) a vector fitting-based [17] time-domain model (VF-TD). The trapezoidal rule of integration, with a time-step of 3.08  $\mu$ s, is used in the SW-TD approach to solve (3). The VF-TD approach consists on first approximating each FD spectrum of the GTFs in (10) via rational functions; then, the set of rational functions is transform to state-space representation which is finally solved via numerical integration. The TD simulation scenario is a step response excitation scenario.

Fig. 3a presents the transient waveforms of the output current given by the SW-TD and VF-TD models and compares these transient waveforms with the equivalent currents,  $i_1^e$  and  $i_2^e$ , given by the NLT simulation. Fig. 3b shows the last 20 ms of the simulation. The results of Fig. 3 show that the equivalent signals closely follow the waveform by the SW-TD model at points  $kT + T_i$ . Moreover, Fig. 3b shows equivalent signals enveloping the original signal.

Fig. 3 also shows a good agreement between VF-TD and NLT simulations. Two notes about these simulations. Due to its intrinsic characteristics, the NLT simulation requires a large number of samples (for this case study 4096 samples) to achieve a precise visualization of the transient waveform, nonetheless it yields more accurate results than the VF-TD simulation. On the other hand, the VF-TD simulation represents a sequential simulation, overcoming the issue of number of samples. Furthermore, VF-TD simulation model may be readily embedded into EMT-type software tools. The

presented results verify the correctness of the model and the underlying concepts.

The cpu-times by SW-TD, NLT, and VF-TD are 0.0155 s, 0.043 s, and 3.48 s, respectively. As for VF-TD, the orders of the approximations are 14 for both  $GTF_{11}$  and  $GTF_{21}$ , and 2 for both  $GTF_{12}$  and  $GTF_{22}$ . Note that, despite the large number of samples, NLT behaves computationally similar to SW-TD.

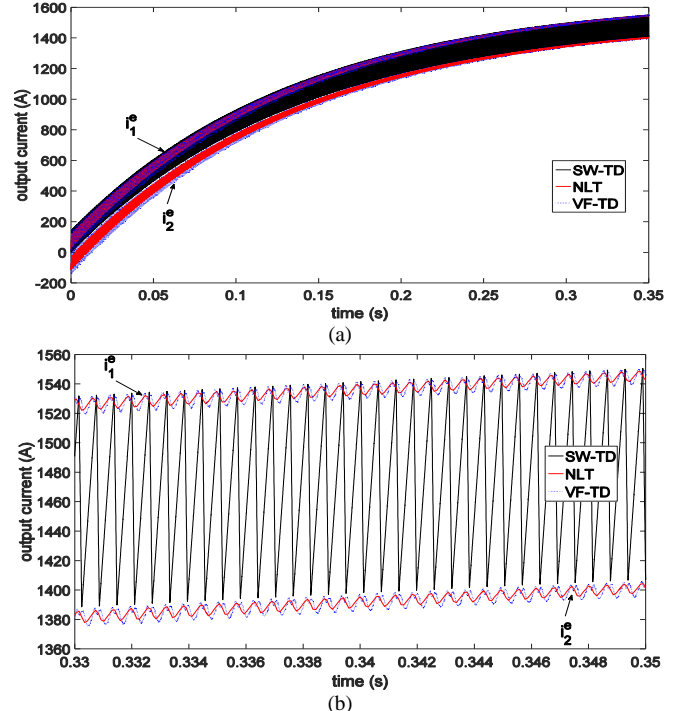


Fig. 3. (a) Transient output current by the SW-TD and VF-TD models and by the NLT simulation, (b) Close-up.

Finally, the stationary state of the equivalent currents,  $i_1^e$  and  $i_2^e$ , is calculated with the NLT method by assuming the damping term of the complex frequency  $s = c + j\omega$  close to zero [15], e.g.,  $10^{-6}$ , and using few samples, e.g., 32. Fig. 4 presents the steady-state of the equivalent currents given by the NLT simulation, compared to the transient waveform by the SW-TD model. Fig. 4b shows the last 30 ms of the simulation. It is worth mentioning that the computation of stationary state via NLT is straightforward while TD-based methods, such as SW-TD and VF-TD, require that the transient dies out resulting in long simulation times. On another note, considering the rational function approximation provided by VF for one of the GTFs, viz.  $GTF_{11}$ , Fig. 5 shows poles and zeros locations for this approximation. The system is critically stable with poles lying on the imaginary access. For the system considered lacks any form of feedback control, the presence of some sort of feedback control implies the movement of the poles towards the zeros, resulting in the system crossing into instability condition.

## V. GENERAL CASE: N-SWITCHING PHASES HBC

The general case of  $N$  switching phases, which results from a switching pattern given by PWM scheme, is illustrated in this section. The parameters of the HBC in Fig. 1, now under  $N$ -switching phase case, are the same as those for the two-switching phase case. Considering a modulating signal with an

amplitude of 0.9, the PWM waveforms presented in Fig. 6 are obtained. This results in  $N = 54$  switching phases. For simplicity, PWM switching is assumed constant during the simulation, i.e., open-loop behavior.

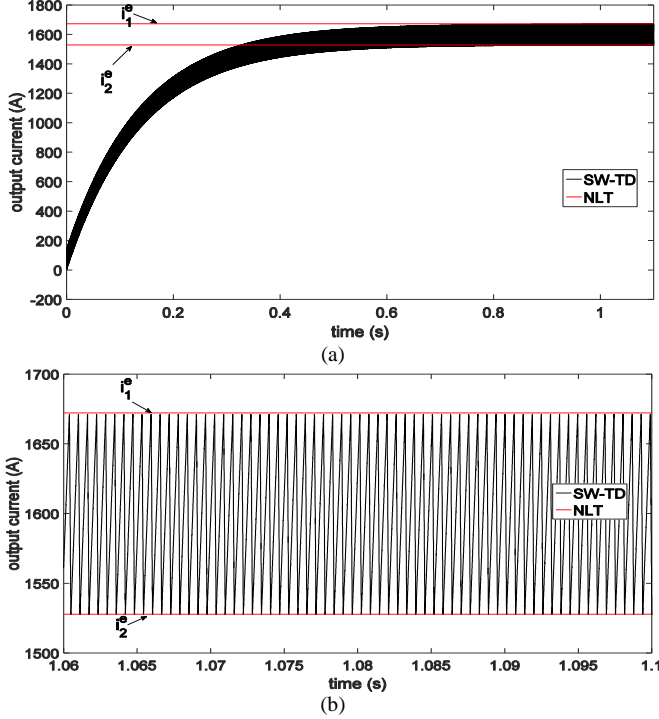


Fig. 4. (a) Steady-state of equivalent currents by the NLT simulation, (b) Close-up.

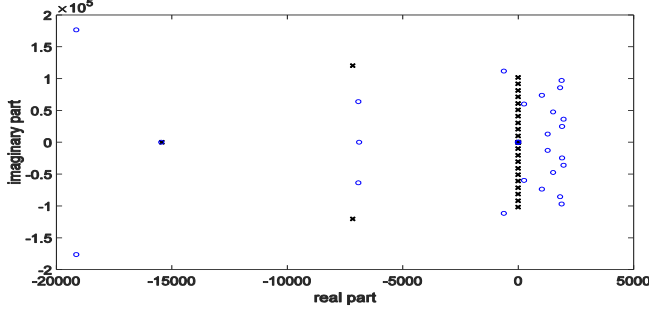


Fig. 5. Pole/zero location for  $GTF_{11}$  approximation as given by VF.

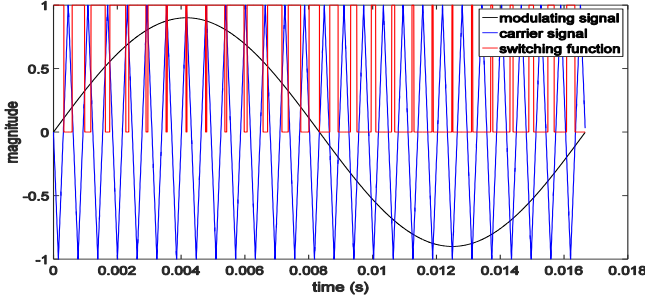


Fig. 6. Waveforms involved in the PWM scheme.

It can be shown that an analytical solution of (8) exists and is given by

$$I_k^e(s) = \frac{b_1 a_2 a_3 \cdots a_k - b_2 a_3 a_4 \cdots a_k + \cdots (-1)^{k-1} b_k}{(-1)^{k-1} + a_1 a_2 \cdots a_k}, \quad (11)$$

where:  $a_k = -g_k e^{-d_k T_s}$ ,  $b_k = G_k [(-1)^k V_{in}(s) - V_s(s)]$ .

The solution of (8), as given by (11), provides the GTFs relating equivalent currents with the two input sources  $V_{in}(s)$

and  $V_s(s)$ . The GTF matrix corresponding to (10) is now of dimensions  $54 \times 2$ .

#### a) FD characterization

The magnitude and phase of the (1, 1), (54, 1), (1, 2) and (54, 2) elements of the GTF matrix are presented in Fig. 7 for a frequency range of 1 Hz to 20 kHz. Similar results are obtained for the rest of the GTFs and thus are not shown here. Fig. 7a shows that for the  $N$ -switching phases case major effect spikes appear around both modulating and switching frequencies and their corresponding multiples. This supports that the developed GTFs capture the system dynamics including those stemming out of switching.

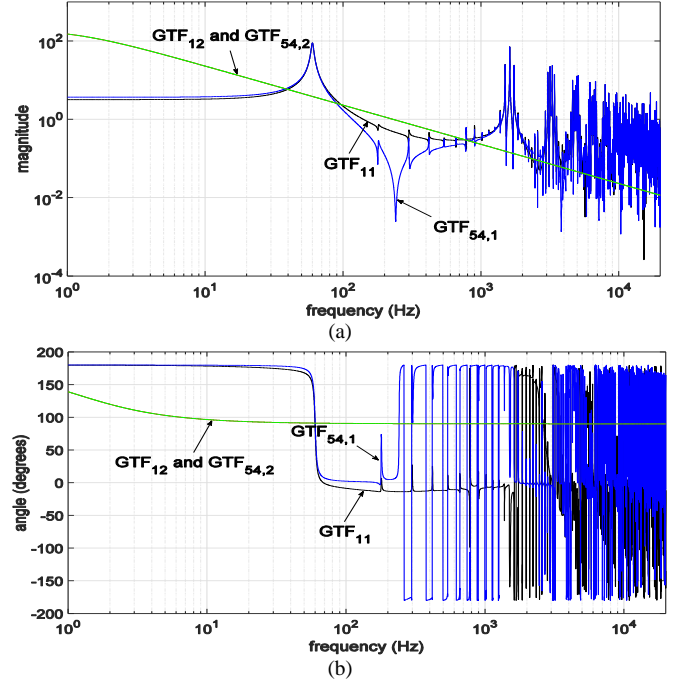


Fig. 7. Four GTFs of 54-switching phases HBC (a) Magnitudes and (b) Phases.

For this case study, the  $s$ -domain pole locations of both the first and second columns of the GTF matrix, i.e., respectively related to  $V_{in}(s)$  and  $V_s(s)$ , correspond to  $-1/\tau$ . The  $z$ -domain zeros and poles are identical for all GTF matrix elements and correspond to the product  $g_1 g_2$ , i.e., 0.9955.

#### b) TD verification

For this case study, the set of the  $N$  equivalent signals in (8) is obtained with the NLT method and compared with the SW-TD model only, as presented in Fig. 8a for the total simulation time and in Fig. 8b for the last 20 ms of simulation. Fig. 8 clearly shows the behavior of the 54 equivalent signals (denoted by dashed-line type) as envelopes of the original signal. The close-up depicted in Fig. 8b shows equivalent signals enveloping the original signal and intersecting with the original signal at the switching instances according to equivalent signal theory. For this case study, the cpu times by SW-TD and NLT are 0.01 s and 0.32 s, respectively, which in turn verifies the accuracy of GTFs and the underlying model. However, for an actual converter PWM, changes during the starting period till it reaches a steady state, which is ignored in this simulation study.

Finally, the stationary state of all equivalent signals for the  $N$ -switching phase case, obtained via NLT, is presented in Fig. 9. Similar to the transient case scenario, the 54 equivalent

signals are denoted by dashed-line type. Worth mentioning the fact that availability of numerical techniques, such as NLT, permits to go beyond the traditional 2-switching phase case presented in existent literature. Moreover, complete FD/TD characterization has not been presented as in this paper.

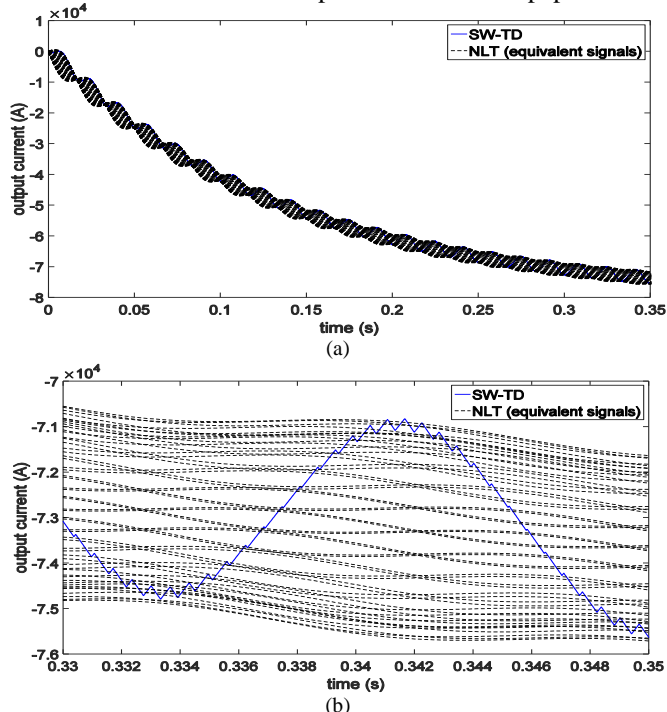


Fig. 8. (a) Transient output current by the SW-TD model and by the NLT simulation, (b) Close-up. — SW-TD, - - - NLT

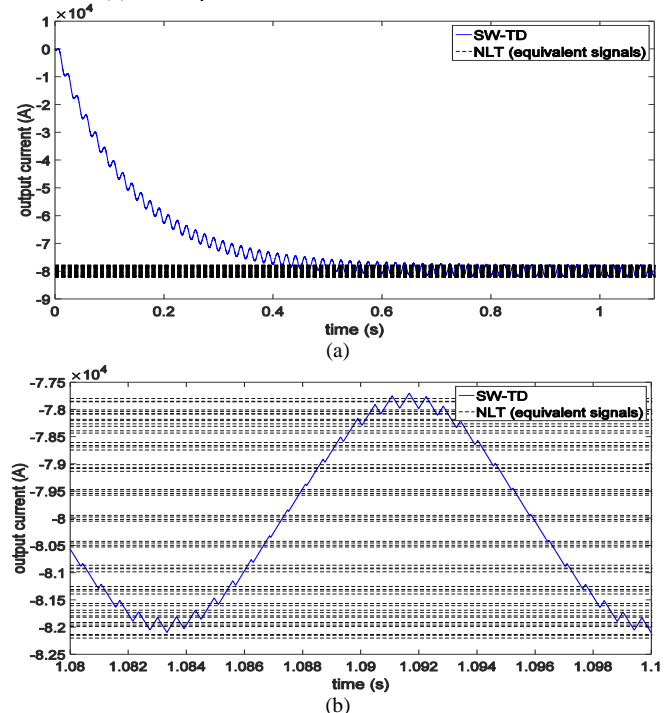


Fig. 9. (a) Steady-state of equivalent currents by the NLT simulation, (b) Close-up.

## VI. CONCLUSIONS

This paper presents preliminary research on the extension of equivalent signal theory and the generalized transfer functions (GTFs) concept to obtain a special class of FD models of

switched circuits mainly used in the power systems area; the HBC is used to illustrate the approach. The developed GTFs provide the FD relationship between the equivalent signals, which pass by specific instances of the output, and the input. Based on the GTF theory, the equivalent signals envelope the output of the modeled device. The approach is applied, in open-loop fashion, on a single-phase HBC under full-wave and PWM switching schemes. In addition to the application of the GTF theory to PWM switching scheme, a thorough analysis in time and frequency domains has been presented. It is shown that the developed GTF HBC model is successful in capturing the system dynamics including switching. Verification of the induced models is achieved by TD simulation. Subsequent research is going to be focused on application of GTFs on power electronic converters of modern power systems aimed at stability analysis and control design as GTFs give access to zeros/poles in both  $s$ - and  $z$ -domain.

## VII. REFERENCES

- [1] H. W. Dommel, *Electromagnetic Transients Program Reference Manual (EMTP Theory Book)*. Portland, OR, USA: Bonneville Power Administration, 1986.
- [2] L. Wei-Xing and D. Jovcic, "High-power high-frequency converter modelling using Dommel's and Runge-Kutta methods in ABC and DQ frame," *Proc. IEEE PES General Meeting 2014*, pp. 1-5, July 2014.
- [3] P. Lehn, "Sensitivity to simulation method for power electronic circuits," *Proc. IEEE PES Summer Meeting 2001*, pp. 1-5, 2001.
- [4] S.R. Sanders, J.M. Noworolski, X.Z. Lui, and G.C. Verghese, "Generalized averaging method for power conversion circuits," *IEEE Trans. on Power Electron.*, vol. 6, pp. 251-259, Apr. 1991.
- [5] M. Mahmoud, A.R. Mohamed, and S. Abdel-Mohaimen, "FPGA-based real-time digital simulation," *Proc. of the International Power Systems Transients (IPST-2005)*, pp. 19-23, 2005.
- [6] J.J. Rico, M. Madrigal, and E. Acha, "Dynamic harmonic evolution using the extended harmonic domain," *IEEE Trans. Power Del.*, vol. 18, no. 4, pp. 587-594, Apr. 2003.
- [7] T. Noda, A. Semlyen, and R. Iravani, "Harmonic domain dynamic transfer function of a nonlinear time-periodic network," *IEEE Transactions on Power Delivery*, Vol. 18, No. 4, pp. 1433-1441, October 2003.
- [8] Y. Tsvividis, "Representation of sampled-data signals as functions of continuous time," *Proc. of the IEEE*, vol. 17, no. 1, Jan. 1983.
- [9] D. Birolek and K. Zaplatilek, "Frequency domain analysis of switched networks by generalized transfer functions," *Proc. of the ECCTD '93*, Davos, Switzerland, pp. 957-962, 1993.
- [10] D. Birolek, "Modeling of periodically switched networks by mixed  $s$ - $z$  description," *Proc. Int. AMSE Conference "Systems Analysis, Control&Design"*, pp. 199-210, Lyon (France), July, 1994.
- [11] D. Birolek, V. Biolkova, and J. Dobes, "Modeling of switched DC-DC converters by mixed  $s$ - $z$  Description," *Proc. of the Int. Symposium on Circuits and Systems*, pp.831-834, Island of Kos, Greece, May, 2006.
- [12] D. Birolek, "Modeling of periodically switched networks by mixed  $s$ - $z$  description," *IEEE Trans. on Circuits and Systems-I: Fundamental Theory and Applications*, vol. 44, no. 8, pp. 750-758, August 1997.
- [13] D. Birolek, "S-z semi-symbolic simulation of switched networks," *Proc. of the IEEE Int. Symposium on Circuits and Systems*, Hong Kong, pp. 1748-1751, 1997.
- [14] D. Birolek and J. Dobes, "Computer simulation of continuous-time and switched circuits: Limitations of SPICE-family programs and pending issues," *Proc. of the 17th Int. Conf. Radioelektronika*, pp. 1-11, Brno, Czech Republic, April 2007.
- [15] P. Moreno and A. Ramirez, "Implementation of the numerical Laplace transform: a Review," *IEEE Trans. on Power Delivery*, vol. 23, no. 4, pp. 2599-2609, October 2008.
- [16] N. Mohan, T.M. Undeland, and W.P. Robbins, *Power Electronics: Converters, Applications, and Design*, John Wiley & Sons Inc., 3<sup>rd</sup> Ed., USA, 2003.
- [17] B. Gustavsen and A. Semlyen, "Rational approximation of frequency domain responses by Vector Fitting," *IEEE Trans. Power Del.*, vol. 14, no. 3, pp. 1052-1061, Jul. 1999.